How well can an amoeba climb?

Yoshio Fukui*†‡, Taro Q. P. Uyeda§, Chikako Kitayama§, and Shinya Inoué†

*Cell and Molecular Biology, Northwestern University Medical School, Chicago, IL 60611-3008; §Biomolecular Research Group, National Institute for Advanced Interdisciplinary Research, Tsukuba, Ibaraki 305-8562, Japan; and †Marine Biological Laboratory, Woods Hole, MA 02543-1005

Contributed by Shinya Inoué, June 22, 2000

We report here our efforts to measure the crawling force generated by cells undergoing amoeboid locomotion. In a centrifuge microscope, acceleration was increased until amoebae of *Dictyostelium discoideum* were "stalled" or no longer able to "climb up." The "apparent weight" of the amoebae at stalling rpm in myosin mutants depended on the presence of myosin II (but not myosins IA and IB) and paralleled the cortical strength of the cells. Surprisingly, however, the cell stalled not only in low-density media as expected but also in media with densities greater than the cell density where the buoyant force should push the amoeba upward. We find that the leading pseudopod is bent under centrifugal force in all stalled amoebae, suggesting that this pseudopod is very dense indeed. This finding also suggests that directional cell locomotion against resistive forces requires a turgid forward-pointing pseudopod, most likely sustained by cortical actomyosin II.

Generation of mechanical forces is essential for cell locomotion, division, embryonic development, and morphogenesis (1–5). Although the forces involved in some of these biological activities have been measured as mechanical properties in *local* regions of living cells (6–9), few measurements have been made of the maximum ability of an *entire* cell to propel itself. An example includes the maximum propulsive force of 7×10^3 pN generated by a swimming ciliated protozoan, *Paramecium caudatum*, measured by using a centrifuge microscope (10). Little is known, in particular, of the propulsive forces that can be generated by any cell undergoing amoeboid movement.

In the present paper, we report the maximum "apparent weight," or centrifugal force against which wild-type and myosin mutants of *Dictyostelium discoideum* amoebae were able to crawl "upward." The small mass of the amoebae required the use of a recently developed centrifuge polarizing microscope capable of generating fields of greater than $11{,}465 \times g$ (Earth's gravitational acceleration), with image resolution of better than 1 μm in differential interference or Nomarsky contrast microscopy (11).

As described below, mutant amoebae stall or cease to be able to crawl up against the imposed apparent weight at characteristic centrifugal accelerations, so they are at least able to overcome that much external force. Those lacking the muscle type myosin, myosin II, stall at very much lower centrifugal acceleration.

However, we will show that the mechanism of stalling, or inability of the amoeba to maintain directional locomotion against the centrifugal field, in fact depends on the very high local density of its leading pseudopod rather than the apparent weight felt by the whole amoeba. Even in media whose density is greater than that of the whole amoeba, amoebae lacking myosin II are unable to sustain the forward protrusion of the high-density pseudopod that is apparently needed to sustain directional amoeboid locomotion against the external field.

Materials and Methods

Cells and Cell Culture. *D. discoideum* wild type NC4 (12), axenic strain Ax3 (13, 14), myosin II heavy chain knockout mutant HS1 (*mhcA*$^-$) (15), and a triple myosin knockout mutant A5 (*mhcA*$^-$/*myoIA*$^-$/*myoIB*$^-$) were cultured as described previously (12–15). Before observation, the growth phase cells were washed from medium by centrifugation ($100 \times g$, 1.5 min) and incubated overnight at 18C° in a standard buffer (10 mM NaCl/10 mM KCl/3 mM $CaCl_2$/2.5 mM Pipes, pH 6.8).

Generation of Myosin Knockout Mutants. Generation of a mutant cell line (A5) that lacks heavy chain genes for myosin II, myosin IA, and myosin IB will be described in detail elsewhere (C.K. and T.Q.P.U., unpublished work). Briefly, a plasmid carrying *Dictyostelium* myosin II heavy chain gene (15) was modified such that a fragment corresponding to the carboxyl quarter of the motor domain and the amino half of the tail were replaced with a blasticidin resistance cassette. The DNA fragment of the disrupted gene was excised and electroporated into a cell line lacking myosins IA and IB (16). Blasticidin resistant colonies were isolated, and the double-crossover gene disruption was confirmed by Southern hybridization. Absence of myosin II heavy chain was further confirmed by Western blot and phenotypic assays.

Centrifuge Polarizing Microscope. The centrifuge polarizing microscope was designed by S.I. and developed in collaboration with Hamamatsu Photonics (Hamamatsu City, Japan) and Olympus Optical Company (Tokyo) (11). Cells were suspended in standard buffer and allowed to settle on the strain-free glass cover of the centrifuge observation chamber. The image of the specimen spinning in the rotor (at a radius of 7.5 cm) at up to 11,700 rpm is frozen stroboscopically by brief (6-ns) laser flashes that illuminate the specimen as it transits between the stationary condenser and objective lenses. The 532-nm wavelength image, formed by a $\times 40/0.55$ numerical aperture objective lens, was captured at video rate by a Hamamatsu interference-fringe-free CCD camera. The original image was recorded into Sony ED-Beta tapes as Y/C signals at video rate through a digital signal converter (Sony model DSC-1024G).

Calibration of Medium Density. The density of stock and diluted Percoll solution (17) (Amersham Pharmacia Biotech) was calculated from the equations below:

$$\rho_{100} = (V_a \times \rho_a) + (V_b \times \rho_b)/(V_a + V_b)$$
$$\rho_i = (V_{100} \times \rho_{100}) + (V_b \times \rho_b)/(V_{100} + V_b)$$

Where

V_a = volume of 23% (v/v) Percoll (from bottle).
V_b = volume of $\times 20$ standard buffer (appropriately diluted to provide final $\times 1$ standard buffer).
V_{100} = volume of stock Percoll (21.85%).

ρ_a = density of 23% (v/v) Percoll = 1.130 gram/cm^3.
ρ_b = density of $\times 20$ standard buffer = 1.005 gram/cm^3.
ρ_{100} = density of stock Percoll = 1.124 gram/cm^3.
ρ_i = density of diluted Percoll.

‡To whom reprint requests should be addressed at: Cell and Molecular Biology, Ward 7-342, Northwestern University Medical School, 303 East Chicago Avenue, Chicago, IL 60611-3008. E-mail: y-fukui@northwestern.edu.

The publication costs of this article were defrayed in part by page charge payment. This article must therefore be hereby marked "*advertisement*" in accordance with 18 U.S.C. §1734 solely to indicate this fact.

Table 1. Apparent weight and stalling rpm for wild-type and myosin knockout mutants in *Dictyostelium*

Cell lines*	NC4	Ax3	HS1	A5
Calculation of reduced mass of amoebae				
Volume† ($\times 10^{-10}$ cm^3)	3.78 ± 1.44	4.87 ± 1.80	4.26 ± 1.34	4.87 ± 1.69
Density‡ (gram/cm^3)	1.066	1.065	1.063	1.063
ΔMass§ ($\times 10^{-11}$ gram)	2.31 ± 0.70	2.92 ± 0.70	2.47 ± 0.78	2.82 ± 0.98
Apparent weight at stalling rpm¶				
Maximum rotation, rpm	>11,700	6,400	3,500	3,400
Stalling acceleration (×g)	>11,465	3,431	1,025	968
Apparent weight at Stall‖ ($\times 10^3$ pN)	>2.59 ± 0.78	0.99 ± 0.24	0.25 ± 0.08	0.27 ± 0.09

The apparent weight was calculated by multiplying the amoeba's reduced mass and the stalling acceleration. The stalling acceleration was calculated from the rpm beyond which the amoebae were unable to crawl centripetally and the distance (7.5 cm) between the center of the rotor to the center of the observation chamber.
*NC4: wild type (12), Ax3: axenic strain (13, 14), HS1: myosin II knockout (*mhcA*$^-$) (15), A5; triple knockout (*mhcA*$^-$/*myoIA*$^-$/*myoIB*$^-$).
†Calculated from measurements of radii of 200 cells each; each cell was assumed to be a 5-μm-high disk.
‡Apparent cell density (δ) was determined as isopycnic density (17).
§ΔMass; reduced mass = (cell density − medium density) × cell volume. Medium density of the standard buffer (ρ_o) was 1.005 gram/cm^3 as measured with an Ostwald's pycnometer (21).
‖(ΔMass) × (stalling acceleration); standard deviation, each based on measurements of radii of 200 cells.

Calibration of Apparent Weight of Amoeba. The forces on the amoebae were calibrated by Newton's equation of motion as below:

$$\text{Force (F)} = \Delta m \times a \times 10^7 (\text{pN}).$$

Where Δm (reduced mass) = [cell density (δ) − medium density (ρ)] × cell volume (gram/cm^3).

$$\text{Acceleration } (a) = \{(2\pi \times R/60)^2 \times r\} \text{ (cm/sec}^2).$$

Where R = rpm and r = distance between the center of the centrifuge rotor and center of the specimen chamber (in centimeters).

Cell density was measured by linear density gradient centrifugation. A 0.5-ml aliquot of cell suspension (2×10^7 cells/ml in the standard buffer) was loaded on a preformed Percoll gradient. The gradient was made by centrifugation of 23% Percoll (ρ = 1.130 gram/cm^3) (17) in silicone-coated Ultra-Clear centrifuge tube (Beckman Coulter) at 20,000 × g for 30 min in an angle-head rotor (JA-20) on a J2–21 M centrifuge (Beckman Coulter). The apparent densities were calibrated by using Density Marker Beads (Amersham Pharmacia Biotech).

Calculation of Equivalent Actin Concentration. The actin concentration (Ai) with densities equivalent to Percoll solutions was calculated by the following equation:

$$\text{Ai} = (\rho_i - \rho_0) \times 1.2/50 \text{ mM}$$

Where ρ_i = density of diluted Percoll at 0, 10, 25, 50, 75, and 100% fraction.

$$\rho_0 = \text{density of actin buffer}$$

Because 50 mg/cm^3 monomeric actin should give rise to 1.2 mM concentration (18), the actin concentrations equivalent to 0–100% Percoll fractions would be 0.12, 0.17, 0.62, 1.4, 2.1, and 2.9 mM (see Table 2 and Fig. 3).

Fluorescence Microscopy. The cells were fixed in methanol containing 1% formalin at −15°C for 5 min and stained with 3 μM tetramethylrhodamine isothiocyanate-phalloidin (rh-ph) (#R-415; Molecular Probes) for 30 min at 36°C. The sample was observed under an epifluorescence microscope (Axioskop-50; Zeiss) equipped with an oil-immersion ×63 plan apo objective (numerical aperture 1.4). The image was acquired with a cooled CCD (PXL; Photometrics, Tucson, AZ) equipped with a Kodak KAF 1400 chip. The fluorescence and phase-contrast images were acquired at an 8-bit depth of gray scale by using an integrated image acquisition and processing system (MetaMorph; Universal Imaging Corporation, West Chester, PA). The spatial resolution of the system is calculated to be better than 250 nm (19, 20).

Results

Behavior of Cells Under High Centrifugal Fields. In the centrifuge polarizing microscope, the glass windows of the specimen chamber lie in the plane of rotation of the rotor. After amoebae that had settled on a glass window started to migrate randomly, we gradually increased the rotational speed (in rpm) of the centrifuge until no amoebae were crawling upward, i.e., against the centrifugal field. At that "stalling" rpm, we found that the amoebae could crawl only sideways or downward. In those amoebae that started to stretch their pseudopods upward and attempted to crawl in that direction, the extended pseudopods would not remain straight up but became bent. The amoebae thereupon started crawling either sideways or downward. Others lost hold of the substrate and fell to the bottom of the centrifuge chamber. The stalling rpm was surprisingly uniform for amoebae of each strain; at only 100 rpm above the stalling rpm, essentially no amoeba was able to crawl upward.

Thus we measure the stalling rpm as the rpm of the centrifuge in which the cell's geometric center (centroid) fails to move centripetally. Because the cells are attached to the glass substrate aligned parallel to the centrifugal field, we calculated the forces on the amoeba at stalling rpm as (reduced mass of the amoeba) × (the centrifugal acceleration/g), where g = 980 cm/sec^2 (see *Materials and Methods* for details). Except in those cases noted, we found that all cell lines were able to remain adherent to the glass surface up to maximum rotation of the centrifuge polarizing microscope.

Apparent Weight of Amoeba at Stalling rpm. Table 1 shows the reduced mass of the amoebae and centrifugal forces (= apparent weight) at which different strains of amoebae were stalled. We found that wild-type amoebae (NC4) (12) could still migrate centripetally under maximum centrifugation. Under this condition, an NC4 amoeba must generate more than 2.59×10^3 pN of

CELL BIOLOGY

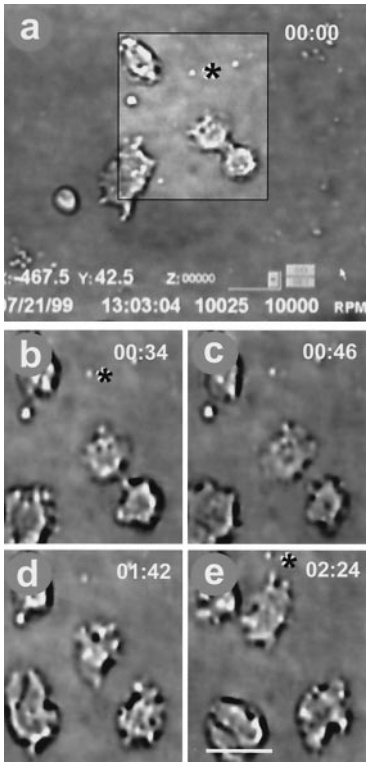

Fig. 1. Behavior of cells under high centrifugal fields. A representative centrifuge microscope image in differential interference or Nomarski contrast showing a wild type NC4 cell undergoing cytokinesis at 10,000 rpm (8,376 × *g*). (*a*) The full video screen; (*b*–*e*) a region of interest extracted sequence acquired at elapsed times indicated (*Upper Right* corner, *a*–*e*). After dividing, the upper daughter cell migrated centripetally. A movie showing the full sequence can be seen in the supplementary material (www.pnas.org). *, stable marker on the substrate. Elapsed time, minute/second. Bar = 5 μm.

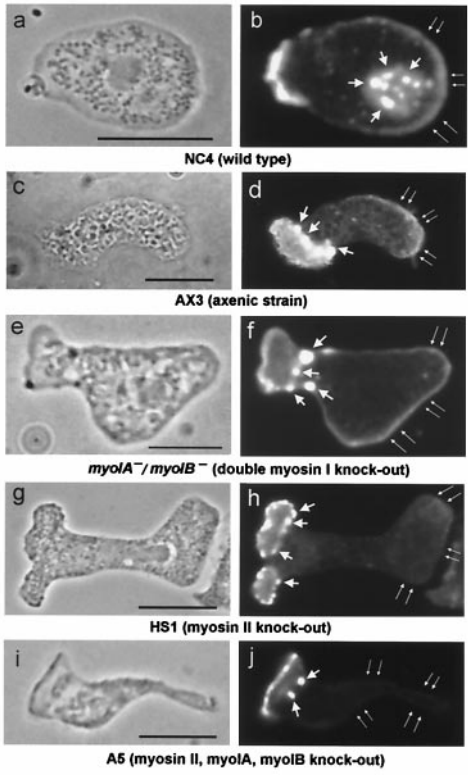

Fig. 2. Distribution of filamentous (F-) actin in migrating *Dictyostelium* amoebae. (*Left*) Phase-contrast images; (*Right*) rhodamine–phalloidin fluorescence. (*a* and *b*) Wild type (NC4) (12); (*c* and *d*) axenic strain (Ax3) (13, 14); (*e* and *f*) double myosin I knockout (*myoIA*$^-$/*myoIB*) (16); (*g* and *h*) myosin II knockout (HS1) (15); (*i* and *j*) triple myosin knockout (A5) strains. Note that the trailing cortex of NC4, Ax3, and *myoIA*$^-$/*myoIB*$^-$ contains a substantial F-actin layer (double thin arrows, *b*, *d*, and *f*). In contrast, the cortical F-actin in myosin II knockout cells (HS1 and A5) is weak (*h* and *j*). The globular fluorescence dots (thick short arrows) represent the cell-substrate anchoring structures ''eupodia'' (19, 20), which are similar to ''podosomes'' or ''invadopodia'' in invasive mammalian cells (30, 31). In contrast to the trailing cortex, actin in the eupodia and leading pseudopod is well established in all five strains. Bar = 5 μm.

climbing force to overcome the downward pull by the centrifugal force. Even so, the wild-type amoebae could divide by apparently normal cytokinesis (Fig. 1) and could even show aggregation behavior (22–24) (video data available as supplementary material; see www.pnas.org).

In contrast to NC4, the axenic strain amoebae (Ax3) (13, 14) stalled at 3,431 × *g*. At higher centrifugal forces, Ax3 cells moved only laterally or centrifugally. The apparent weight of Ax3 at stalling rpm was 0.99×10^3 pN, or less than 40% of NC4. These measurements support the proposition that axenic strains in fact are not wild type but are motility mutants of NC4 (25, 26).

As with Ax3 and NC4, the myosin II knockout mutant (HS1) (15) could remain attached to the substrate up to maximum speed of the centrifuge. This mutant, lacking myosin II, could migrate only laterally or centrifugally and not centripetally at speeds higher than 3,500 rpm (at 1,025 × *g* Table 1 *Lower*). The apparent weight for HS1 at stalling rpm was 0.25×10^3 pN, or 25% of the parental Ax3.

To examine possible contribution from two ''mini''-myosin isoforms (myosins IA and IB), we measured the apparent weight at stalling rpm of a triple myosin knockout mutant (A5) from which myosin IA and IB as well as myosin II were removed. A5 cells were found capable of migrating against the centrifugal field up to 968 × *g*. Under this rpm, the apparent weight of A5 cells (0.27×10^3 pN) against which the cells can generate upward migration forces is similar to that of HS1, indicating that myosin IA and IB do not add extra migration forces to the myosin II knock-out mutant.

The above results indicate that the ability of *Dictyostelium* amoebae to generate forces that counter their apparent weight are myosin II dependent to a major extent. In this context, we note that the ratio of apparent weight at stalling rpm in the myosin II knockout mutant to the parental strain Ax3 (i.e., 25%) more or less parallels published ratios of cortical tensions measured by poking with a microneedle (68%; ref. 6) or sucking with a microcapillary (50%; 7, 30%; ref. 8). Because myosin II is reported to be localized in the posterior (trailing) cortex of *Dictyostelium* amoebae (4, 27–29), we next examined the organization of cortical F-actin (the major constituent of the cortex) in those mutants whose stalling we observed.

Weak F-Actin Cortex in Myosin II Knockout Mutants. By fluorescence microscopy, we find that the cortical F-actin in the layer surrounding the trailing cell body (double thin arrows) is well established in wild-type NC4 (Fig. 2 *a* and *b*), the axenic strain Ax3 (*c* and *d*), and the double myosin I knockout mutant (*myoIA*$^-$/*myoIB*$^-$) (*e* and *f*). However, it is poorly organized in the myosin II knockout mutants (HS1, *g* and *h*; A5, *i* and *j*). In contrast, in the leading pseudopod and the eupodia, F-actin is highly concentrated in all five strains. These results, together with decreased migration forces in HS1 and A5, suggest that the strength of the cortical actomyosin II in the posterior cortex plays an important role in generating directional migration forces in *Dictyostelium*.

Table 2. Medium density vs. stalling acceleration measured in myosin II knockout mutant (HS1)

Fraction of stock percoll, %*	0	10	25	50	75	100
Medium density (gram/cm^3)†	1.005	1.012	1.031	1.062	1.093	1.124
Stalling revolution, rpm	3,500	4,100	4,900	6,800	7,800	8,600
Stalling acceleration, $\times g$	1,025	1,408	2,011	3,873	5,096	6,195
Buoyant force‡ ($\times 10^3$ pN)	−0.25	−0.31	−0.27	−0.02	0.65	1.61

*Percents (v/v) of stock Percoll solution. The stock Percoll was 21.85% of Percoll containing the standard buffer (see *Materials and Methods*).

†Density was calibrated by using Density Marker Beads (17).

‡Calculated using Δmass in various Percoll concentrations. In high-density media, the cells are exposed to buoyant forces in excess of their apparent weight, yet their upward migration is still progressively limited by the centrifugal field (see also Fig. 3).

Stalling in High-Density Medium. If the apparent weights accurately reflect the ability of cells to migrate directionally against an external force, the cells should be able to resist higher centrifugal forces when they are surrounded by media with elevated density and become more buoyant. We find that this assumption is in fact correct. The density of the medium was changed by using various concentrations of Percoll (see *Materials and Methods*). Observations were made on the myosin II knockout mutant (HS1cells) because they stall under moderate centrifugal fields (Table 1 *Lower*).¶

As predicted, the HS1 cells kept migrating centripetally at much higher rpm in Percoll solutions than in standard buffer solution (Table 2*)*. Surprisingly, however, the cells would stall even when exposed to media whose density was higher than the cell's density (Fig. 3). This result was unexpected because in those Percoll solutions, the cells are actually being pushed upward by their buoyancy. In fact, amoebae that became detached in those solutions floated up instead of sinking. In 50% Percoll, the cells should have *no* apparent weight and should be receiving no centrifugal forces even at the maximum rotation because the reduced mass is nearly zero. Beyond 50%, the cells are pushed upward harder when the rotational speed increases (because of increasing buoyant forces). Nevertheless, in 50% Percoll medium, the cells stalled at 3,873 $\times g$ (Table 2). At higher Percoll density, the stalling acceleration continued to rise monotonically, continuing the tendency seen for Percoll densities less than the average density of the amoeba (Table 2, Fig. 3). These results clearly show that the apparent weight at stalling rpm is *not* a simple measure of the maximum directional migration force that the amoebae can generate but must reflect some other event taking place in or on the amoeba.

Bending Pseudopods Under High Centrifugal Fields. As noted, we found that when the cell fails to migrate "upward" against the centrifugal field, a pseudopod protruding upward from the leading cell body is bent down. In fact, this behavior of the pseudopods was observed in all strains when the cells fail to migrate centripetally, *including* in those cells that were exposed to media with elevated density (Fig. 4*A*). Thus it is not the apparent weight, or the centrifugal force applied to the whole amoeba, that determines the stalling rpm. Rather, it is the centrifugal field under which the leading pseudopod is bent that stalls the "upward" directional migration of the amoeba.

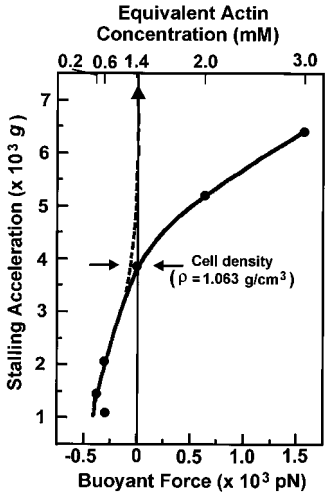

Fig. 3. Relationship between stalling acceleration and buoyant force experienced by amoebae in media with different densities. The stalling acceleration was measured on HS1. After the cells adhered to the glass surface in the centrifuge observation chamber, the medium was replaced with 10, 25, 50, 75, and 100% stock Percoll. Absolute concentrations of Percoll and their densities (ρ) are shown in Table 2. The buoyant force changes from negative to positive when the medium density approaches the cell density (δ = 1.063 grams/cm^3). The graph shows that the cells stall even in media whose density is higher than the average cell density. Dashed line indicates the anticipated result extrapolated from stalling at lower media density, assuming that the apparent weight of the cells determines the stalling acceleration. The actin concentrations (*Upper*) represent calculated actin concentrations whose densities are equivalent to the Percoll solutions (see *Materials and Methods*).

These observations show that the density of the pseudopod itself must be very high indeed (>3 mM equivalent of actin; see Fig. 3). It also suggests that forward protrusion of the pseudopod is a prerequisite for directional amoeboid locomotion.

Discussion and Conclusion

Because those mutant cells lacking myosin II stall at low rpm and also show a weak trailing cortex, we postulate that beyond the stalling rpm their fragile cortex is unable to support the needed upward thrust of the leading pseudopod. We argue that the rigidity of the pseudopod will very likely depend on the circumferential strength of its tubular cortex plus a sufficiently high hydrostatic pressure provided by the actomyosin II-containing contracting cortex surrounding the trailing cell body. If the cortical contracting force is inadequate, the turgor pressure in the cell would be too weak to support the leading pseudopod that is needed to propel the amoeba against a load that has to be overcome (Fig. 4*B*).

In summary we conclude that myosin II, but not myosins IA and IB, plays a crucial role in the generation of cortical contraction forces. Because there are more than 10 myosin I (minimyosin) genes identified in *Dictyostelium* (32), we are unable to decipher the direct or "compensatory" roles (33) of the minimyosins as a whole. Nevertheless, there is no question that the cells lacking myosin II have considerable less ability to generate forward migrating forces.

We believe that the forward protrusion of the leading pseudopod is not simply a phenomenon observed in *Dictyostelium* and other amoebae, but that it is an essential feature for the directional migration of cells undergoing amoeboid locomotion in general (1, 4). Once the direction of propagation is defined by some cue [e.g., cyclic adenosine-3′,5′-monophosphate gradient

¶Under the brief periods of centrifugation required for our observations, we found no signs of Percoll stratification or differences in rpm for the amoebae stalling at various heights within the centrifuge chamber.

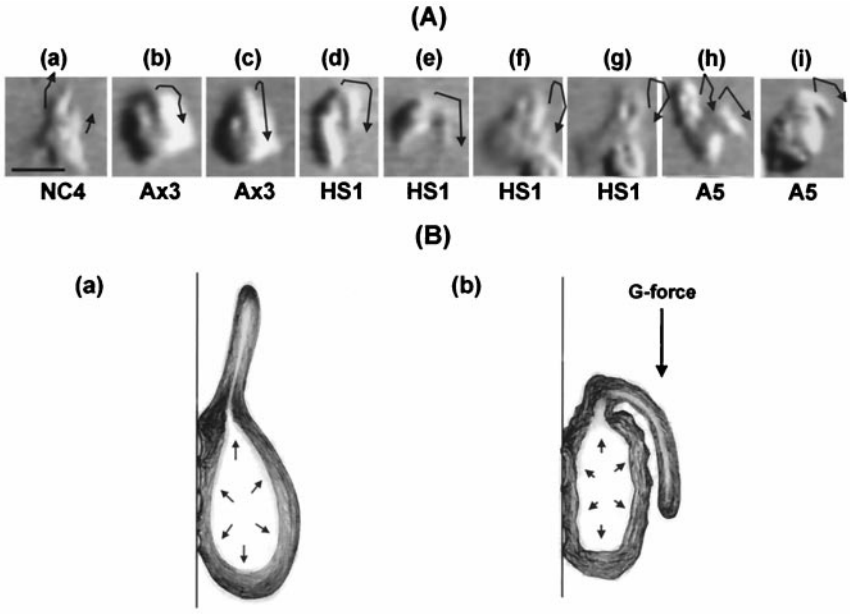

Fig. 4. Behavior of pseudopods and proposed stalling mechanism. (*A*) Selected video frames showing behavior of pseudopods. (*a*) Control. When an amoeba migrates centripetally, the leading pseudopod(s) continues to protrude upward. (*b–i*) At stalling rpm, where the amoebae can no longer migrate against the centrifugal force, the pseudopod(s) bends down. NC4, original wild type; Ax3, parental axenic strain; HS1, myosin II knockout (*mhcA*$^-$); A5, triple myosin knockout (*mhcA*$^-$/*myoIA*$^-$/*myoIB*$^-$). Arrows, approximate shape of pseudopods. Bar = 5 μm. (*B*) Diagram illustrating the suggested stalling mechanism. (*a*) The cortical tension represents a sum of the tangential stress rendered by the cortical structure and the hydrostatic pressure in the cell. Contractile force generated by the cortical actomyosin II, which is bound to the semipermeable plasma membrane, provides a turgor pressure to support a protruding pseudopod. Because the pseudopod is not attached to the substrate and must be supported by the cell body, the cortical F-actin framework must support the protruding pseudopod. (*b*) Lacking myosin II, the cortical F-actin layer cannot produce sufficient hydrostatic pressure to support the forward protrusion of the pseudopod. When the weak cortex cannot provide enough turgor to support the F-actin-rich dense leading pseudopod, it bends down under the strong G-forces generated by the centrifuge. If the bent pseudopod manages to attach to the substrate, the cell can migrate sideways or downward but not upward. Otherwise the cell detaches and falls down or, in media whose density exceeds that of the cell, floats up.

for *Dictyostelium* amoebae (22–24)] and a pseudopod starts forming in that direction (34, 35), we suggest that the contractile force generated by the trailing cell cortex must provide adequate support for the pseudopod to penetrate into that direction without collapsing against the external force, whether gravitational or a barrier presented, for example against leukocytes, parasitic protista, or migrating embryonic cells by a tissue layer.

Although we have learned that the mechanism by which a cell stalls in a centrifugal field is more sophisticated than initially assumed, we believe that the stall forces measured, as apparent weight with a centrifuge microscope, nevertheless provide valid measures for the relative crawling force that an amoeboid cell can generate for *directional* migration. The relative crawling force as well as the stalling acceleration depends on the presence of myosin II (but not myosins IA and IB) which, in association with actin filaments, provides for a robust trailing cortical layer. We postulate that the directional locomotion of an amoeboid cell requires the contractile cortical framework to provide the turgidity needed for the leading pseudopod to direct the locomotion in that direction.

This paper is dedicated to a memory of Prof. Noburo Kamiya (1913–1999), a pioneer in the research of biological forces, who, among other pioneering explorations, devised the ingenious method of the hydrostatic forces needed for cytoplasmic streaming in syncytial slime molds. We thank Hamamatsu Photonics and the Olympus Optical Company for support of this research and Dr. G. Albrecht-Buehler of Northwestern University Medical School, Chicago, Illinois and Dr. I. Mabuchi of the Tokyo University for discussions about biological forces and actin density. We thank Dr. T. D. Pollard of the Salk Institute for careful reading and astute comments on an earlier version of the manuscript and Dr. R. Oldenbourg of the Marine Biological Laboratory (MBL) for discussions on the forces produced by the apparent weight of an object in a centrifuge. We also thank Dr. L. G. Tilney of the University of Pennsylvania for helpful comments on the manuscript. Thanks are also due to R. A. Knudson, J. MacNeil, and D. Baraby of MBL for their technical and secretarial support.

1. Stossel, T. P. (1982) *Philos. Trans. Soc. London B* **299,** 275–289.
2. Pollard, T. D. & Cooper, J. A. (1986) *Annu. Rev. Biochem.* **55,** 987–1035.
3. Spudich, J. A. (1989) *Cell Regul.* **1,** 1–11.
4. Harris, A. K. (1994) *Int. Rev. Cytol.* **150,** 35–68.
5. Borisy, G. G. & Svitkina, T. M. (2000) *Curr. Opin. Cell Biol.* **12,** 104–112.
6. Pasternak, C., Spudich, J. A. & Elson, E. L. (1989) *Nature (London)* **341,** 549–551.
7. Egelhoff, T. T., Naismith, T. V. & Brozovich, F. V. (1996) *J. Muscle Res. Cell Motil.* **17,** 269–274.
8. Dai, J. H., Ting-Beall, P., Hochmuth, R. M. Sheetz, M. P. & Titus, M. A. (1999) *Biophys. J.* **77,** 1168–1176.
9. Oliver, T., Dembo, M. & Jacobson, K. (1999) *J. Cell Biol.* **145,** 589–604.
10. Kuroda, K. & Kamiya, N. (1989) *Exp. Cell Res.* **184,** 268–272.
11. Inoué. S., Knudson, R. A., Suzuki, K., Okada, N., Takahashi, H., Iida, M. & Yamanaka, K. (1998) *Microsc. Microanal.* **4,** 36–37.
12. Raper, K. B. (1935) *J. Agr. Res.* **50,** 135–147.
13. Free, S. J. & Loomis, W. F. (1974) *Biochimie* **56,** 1525–1528.
14. Franke, J. & Kessin, R. (1977) *Proc. Natl. Acad. Sci. USA* **74,** 2157–2161.
15. Egelhoff, T. T., Manstein, D. J. & Spudich, J. A. (1990) *Dev. Biol.* **137,** 359–367.
16. Novak, K. D., Peterson, M. D., Reedy, M. C. & Titus, M. A. (1995) *J. Cell Biol.* **131,** 1205–1221.
17. In *Percoll: Methodology and Applications* (1995) (Pharmacia LKB Biotechnology, Uppsala, Sweden) pp. 5–12.
18. Tilney, L. G. & Inoué, S. (1985) *J. Cell Biol.* **100,** 1273–1283.
19. Fukui, Y. & Inoué, S. (1997) *Cell Motil. Cytoskeleton* **36,** 339–354.
20. Fukui, Y., de Hostos, E. L., Yumura, S., Kitanishi-Yumura, T. & Inoué, S. (1999) *Exp. Cell Res.* **159,** 141–157.
21. Fukui, Y. (1976) *Dev. Growth Differ.* **18,** 145–155.
22. Bonner, J. T. (1947) *J. Exp. Zool.* **106,** 1–26.
23. Gerisch, G. (1982) *Annu. Rev. Physiol.* **44,** 535–552.

24. Devreotes, P. N. (1989) *Science* **245,** 1054–1058.
25. Williams, K. L., Kessin, R. H. & Newell, P. C. (1974) *Nature (London)* **247,** 142–143.
26. Kayman, S. C. & Clarke, M. (1983) *J. Cell Biol.* **97,** 1001–1010.
27. Yumura, S., Mori, H. & Fukui, Y. (1984) *J. Cell Biol.* **99,** 894–899.
28. Yumura, S. & Fukui, Y. (1985) *Nature (London)* **314,** 194–196.
29. Fukui, Y., Lynch, T. J., Brzeska, H. & Korn, E. D. (1989) *Nature (London)* **341,** 328–331.
30. Tarone, G., Cirillo, D., Giancotti, F. G., Comoglio, P. M. & Marchisio, C. (1985) *Exp. Cell Res.* **151,** 141–157.
31. Chen, W.-T. (1989) *J. Exp. Zool.* **251,** 167–185.
32. Titus, M., A., Kuspa, A. & Loomis, W. F. (1994) *Proc. Natl. Acad. Sci. USA* **91,** 9446–9450.
33. André, E., Brink, M. & Gerisch, G. (1989) *J. Cell Biol.* **108,** 985–995.
34. Condeelis, J. (1993) *Annu. Rev. Cell Biol.* **9,** 441–444.
35. Fukui, Y. (1993) *Int. Rev. Cytol.* **144,** 85–127.